EUROGRAPHICS Workshop on Multimedia (2004)
N. Correia, J. Jorge, T. Chambel, Z. Pan (Editors)

A Segmentation Algorithm for Jacquard Images Based on Mumford-Shah Model

Zhilin Feng, Jianwei Yin, Gang Chen, Yang Liu and Jinxiang Dong

State Key Laboratory of CAD & CG, Zhejiang University, P.R. China

Abstract

Automatic pattern segmentation of jacquard images is a challenging task due to the complexity of the images. Active contour models have become popular for finding the contours of a pattern with a complex shape. However, these models have many limitations on the pattern segmentation of jacquard images in the presence of noise. In this paper, a robust algorithm based on the Mumford-Shah model is proposed for the segmentation of noisy jacquard images. We discretize the Mumford-Shah model on piecewise linear finite element spaces to yield greater stability and higher accuracy. A novel iterative relaxation algorithm for the numerical solving of the discrete version of the Mumford-Shah model is presented. During each iteration, we first refine and reorganize an adaptive triangular mesh to characterize the essential contour structure of a pattern. Then, we apply the quasi-Newton algorithm to find the absolute minimum of the discrete version of the model at the current iteration. Experimental results on synthetic and jacquard images have shown the effectiveness and robustness of the algorithm.

Categories and Subject Descriptors (according to ACM CCS): I.4.6 [Segmentation]: Edge and feature detection).

1. Introduction

Image segmentation plays an essential role in jacquard image analysis. An accurate extraction of pattern features from jacquard images promises reliability for jacquard fabric CAD. Although, many algorithms have been proposed for the segmentation problem, they have difficulty in capturing the complex structure of the visual features, such as complex contours of a jacquard pattern. In practice, the strong variability of jacquard patterns, and the low and varying contrast of topological curves in jacquard patterns make it quite difficult to obtain reliable performance with common segmentation methods.

Lately, many active contour models (see, e.g., [CRB99] [KWT87], [MGR04], [MSV95]) are proposed to extract the contour of an object with a complex shape. However, in a jacquard image, consistently strong edge information is not always presented along the entire boundary of the contours to be segmented. Moreover, if the available jacquard image is heavily corrupted by noise, the performance of the active contour models is often inadequate. Recently, these active contour models have been further improved by incorporating statistical model and prior knowledge to provide more accurate segmentation results. Chesnaud *et al.* [CRB99] proposed a probabilistic framework for image segmentation where different probability density functions from the exponential family are allowed. The parameters of the probability function are determined to deform the snake to detect the image regions. Zhuang *et al.* [ZHPZ96] proposed a robust statistical approach for the problem of Gaussian mixture density modeling and decomposition. The approach can be incorporated into the statistic snake framework to achieve a higher robustness for the shape detection from the noise data. Martin *et al.* [MGRG04] analyzed level set implementation of region snakes based on maximum likelihood estimation techniques for different noise models that belong to the exponential family.

Mumford-Shah model (see, e.g., [MS89], [TYW01]) is another popular method for complex pattern segmentation, which is more immune to noise than the active

contour models. It allows a construction of more efficient strategies for detecting discontinuities in the presence of noise. In contrast to the active contour models, this method utilizes not only image information near the evolving contour but also image statistics inside and outside the contour, so it is more suitable for the segmentation of noisy jacquard images. In this paper, we focus on the segmentation of noisy jacquard images using the Mumford-Shah model.

However, the minimization of the Mumford-Shah model poses a difficult numerical problem, since it requires the computation of geometrical properties of the unknown set of discontinuity boundaries. There are many methods for the minimization of the Mumford-Shah model (see, e.g., [AT90], [Cha95], [CV01], [Gob98]). In this paper, we propose an iterative relaxation algorithm to minimize the Mumford-Shah model on piecewise linear finite element spaces. Our algorithm involves two coordinate steps during each iteration: (1) refining and reorganizing an adaptive triangular mesh to characterize the essential contour structure of a pattern, and (2) minimizing the discrete version of the Mumford-Shah model by the quasi-Newton algorithm.

The rest of this paper is organized as follows. In Section 2, we describe the Mumford-Shah model for segmentation. In Section 3, we give some notations and important results on this subject. In Section 4, we give a discrete version of the anisotropic Mumford-Shah model. Section 5 is devoted to the numerical implementation of our algorithm. In Section 6, some experimental results and evaluations are presented. Finally, we give a brief conclusion of this research.

2. The Mumford-Shah model

Let $\Omega \subset R^2$ be a bounded open set and $g \in L^\infty(\Omega)$ represent the image intensity. The function g has discontinuities that represent the contours of objects in the image. The image segmentation problem consists in the detection of such discontinuities with the simultaneous suppression of noise. Mumford and Shah [MS89] proposed a variational method for image segmentation which looks for a piecewise smooth approximation u of the function g, with u discontinuous across a closed set K. The variational problem consists in the minimization of the following functional

$$E(u,K) = \int_{\Omega\setminus K} |\nabla u|^2 \, dx + \alpha \int_{\Omega\setminus K} (u-g)^2 dx + \beta H^1(K) \quad (1)$$

over closed set $K \subset \Omega$ and $u \in C^1(\Omega \setminus K)$. Here, H^1 is the 1-dimensional Hausdorff measure, and α, β are positive weights. By the Mumford-Shah model, the image segmentation problem is then reduced to find a set K of contours decomposing the image into regions and a function u which is piecewise smooth on that decomposition. Here, the first term penalizes strong variations of u, thus ensuring that u is a smooth approximation of g, the second term forces u to be close to the given image g, and the last term prevents the edges from filling up the whole image.

3. Weak formulation and Γ-convergence

3.1 Weak formulation

Heuristically, we expect solutions to Eq. (1) to be smooth and close to the image g at places $x \notin K$, and K constitutes edges of the image. To show existence of solutions to Eq. (1), a weak formulation was proposed by De Giorgi *et al*. [DCL90] by setting $K = S_u$ (the jumps set of u) and minimizing only over $u \in SBV$, the space of special functions of bounded variation. We recall some definitions and properties concerning functions with bounded variation.

Definition 1. Let $u \in L^1(\Omega; R^2)$, we say that u is a function with bounded variation in Ω, and we write $u \in BV(\Omega; R^2)$, if the distributional derivative Du of u is a vector-valued measure on Ω with finite total variation.

Definition 2. Let $u \in L^1(\Omega; R^2)$, we denote by S_u the complement of the Lebesgue set of u, i.e., $x \notin S_u$ if and only if $\lim_{\rho\to 0} \rho^{-n} \int_{B_\rho(x)} |u(y) - z| \, dy = 0$ for some $z \in R^2$, where $B_\rho(x) = \{y \in R^2 : |y - x| < \rho\}$

Definition 3. Let $u \in BV(\Omega)$, we define the three measures $D^a u$, $D^j u$ and $D^c u$ as follows. By the Radon-Nikodym Theorem we set $Du = D^a u + D^s u$ where $D^a u$ is the absolutely continuous part of Du, $D^s u$ is the singular part of Du. $D^s u$ can be further decomposed into the part supported on S_u (the jump part $D^j u$) and the rest (the Cantor part $D^c u$): $D^j u = D^s u|_{S_u}$ and $D^c u = D^s u|_{\Omega\setminus S_u}$. Thus, we can then write $Du = D^a u + D^j u + D^c u$.

Definition 4. Let $u \in BV(\Omega)$, we say that u is a special function of bounded variation, and we write $u \in SBV(\Omega)$, if $D^c u = 0$.

De Giorgi *et al*. [DCL90] gave the weak formulation of the original problem (1) as follows:

$$E(u,K)=\int_{\Omega}|\nabla u|^2\,dx+\alpha\int_{\Omega}(u-g)^2dx+\beta H^1(S_u) \qquad (2)$$

.They also proved that minimizers of the weak problem (2) are minimizers of the original problem (1). However, from a numerical point of view, it is not easy to compute a minimizer for Eq. (2), due to the term $H^1(S_u)$, and to the fact that this functional is not lower-semicontinuous with respect to S_u. It is natural to try to approximate Eq. (2) by simpler functionals defined on *SBV* spaces. Ambrosio and Tortorelli [AT90] showed that Eq. (2) can be approximated by a sequence of elliptic functionals which are numerically more tractable. The approximation takes place in the sense of the Γ-convergence.

3.2 Γ-convergence

To approximate and compute solutions to Eq. (2), the most popular and successful approach is to use the theory of Γ-convergence. This theory, introduced by De Giorgi and Franzoni [Dal93], is designed to approximate a variational problem by a sequence of regularized variational problems which can be solved numerically by finite difference/finite element methods. Note that Γ-convergence is stable under continuous perturbations, and guarantees the convergence of minima and minimizers.

Definition 5. Let X be a metric space, let $\{F_k\}$ be a sequence of functions defined in X with values in R. Let us set

$$\Gamma\text{-}\liminf_{k\to+\infty}F_k(u):=\inf_{u_k\to u}\left\{\liminf_{k\to+\infty}F_k(u_k):\{u_k\}\to u\right\},$$

$$\Gamma\text{-}\limsup_{k\to+\infty}F_k(u):=\inf_{u_k\to u}\left\{\limsup_{k\to+\infty}F_k(u_k):\{u_k\}\to u\right\}.$$

If $\Gamma\text{-}\liminf_{k\to+\infty}F_k(u)=\Gamma\text{-}\limsup_{k\to+\infty}F_k(u)=F(u)$ for all $u\in X$, we say that F is the Γ-limit of $\{F_k\}$, and we write $F(u)=\Gamma\text{-}\lim_{k\to+\infty}F_k(u)$.

De Giorgi *et al*. [Dal93] proved that

Theorem 1. Assume F_k Γ-converges to F and for every k, let u_k be a minimizer of F_k over X. If the sequence (or a subsequence) u_k converges to some $u\in X$, then u is a minimizer for F and $F_k(u_k)$ converges to $F(u)$.

So, we can say that a family $\{F_\varepsilon\}_{\varepsilon>0}$ of functions Γ-converges to F as $\varepsilon\to 0^+$, if $\{F_{\varepsilon_j}\}$ Γ-converges to F for every sequence $\{\varepsilon_j\}\to 0^+$.

4. Discrete functional of numerical approximation

Now we consider the numerical approximation, in the sense of Γ-convergence, by a sequence of discrete functionals defined on finite elements spaces over structured and adaptive triangulation. Let $\Omega=(0,1)\times(0,1)$, let $\mathcal{T}_\varepsilon(\Omega)$ be the triangulations and let ε denote the greatest length of the edges in the triangulations. Moreover let $V_\varepsilon(\Omega)$ be the finite element space of piecewise affine functions on the mesh $\mathcal{T}_\varepsilon(\Omega)$, let $\{\mathcal{T}_{\varepsilon_j}\}$ be a sequence of triangulations with $\varepsilon_j\to 0$ and let $f:[0,+\infty)\to[0,+\infty)$ be a non-decreasing continuous function such that $\lim_{t\to 0}\frac{f(t)}{t}=1$ and $\lim_{t\to+\infty}f(t)=f_\infty<+\infty$.

Negri [Neg99] proved that

Theorem 2. For each sequence of triangulations $\{\mathcal{T}_{\varepsilon_j}\}$ there exists a convex, 1-homogeneous function $\phi:R^2\to[0,+\infty)$ such that the functional

$$F_{\varepsilon_j}(u,T)=\frac{1}{\varepsilon_j}\int_{\Omega}f(\varepsilon_j|\nabla u_T|^2)dx+\int_{\Omega}(u_T-g)^2dx \qquad (3)$$

Γ-converges respect to strong L^2- topology to the anisotropic Mumford-Shah model

$$F(u)=\int_{\Omega}|\nabla u|^2\,dx+f_\infty\int_{S_u}\phi(v_u)dH^1+\int_{\Omega}(u-g)^2dx \qquad (4)$$

We choose $f(x)=\frac{2\beta}{\pi}\arctan(\frac{\pi x}{2\beta})$, and define the minimizing discrete model as follows:

$$F_{\varepsilon_j}(u,T)=\alpha\int_{\Omega}(u_T-g)^2dx+\frac{1}{\varepsilon_j}\int_{\Omega}\frac{2\beta}{\pi}\arctan(\frac{\pi\varepsilon_j}{2\beta}|\nabla u_T|^2)dx \qquad (5)$$

By theorem 2, we know that Eq. (5) Γ-converges to

$$F(u)=\int_{\Omega}|\nabla u|^2\,dx+\alpha\int_{\Omega}|u-g|^2\,dx+\beta\int_{S_u}\phi(v_u)dH^1 \qquad (6)$$

where v_u is a unit normal to S_u. Eq. (6) is an anisotropic version of Eq. (2), and the function ϕ is applied to take into account the anisotropy introduced by the geometry of the triangulation T.

5. Numerical implementation

In order to arrive at the joint minimum (u,T) of Eq. (5), we propose an iterative relaxation algorithm to implement the numerical solving of Eq. (5). Fig.1 illustrates the outline of the proposed algorithm.

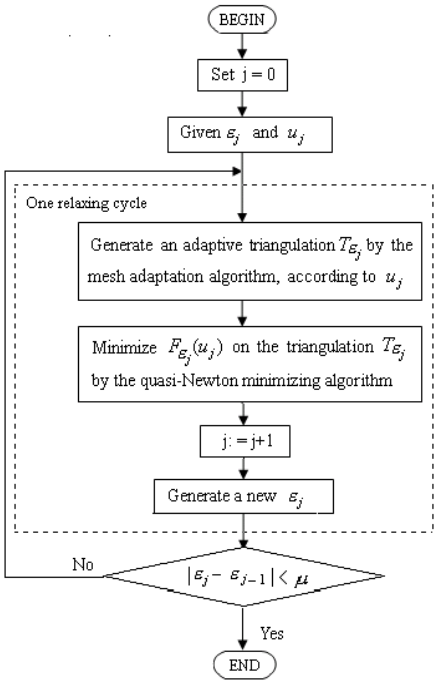

Figure 1: *Outline of the proposed algorithm.*

The main idea of the proposed algorithm is as follows: alternating back and forth between minimizing Eq. (5) holding T constant and adapting triangulation T holding u constant. The intuitive idea behind the algorithm is that if the triangulation T were known and held constantly, it would be straightforward to calculate the variable u, and if the variable u were known, it would be straightforward to calculate the triangulation T. During each iteration, a scheme for the mesh adaptation is first enforced to refine and reorganize a triangular mesh to characterize the essential contour structure. Then, the quasi-Newton algorithm is applied to find the absolute minimum of the discrete version of the functional at the current iteration.

5.1 Mesh adaptation algorithm

There are several approaches to refine and reorganize an existing triangulation. Delaunay triangulation algorithms have been used successfully for unstructured mesh generation. In this paper, we use the Delaunay type mesh generator BL2D [BL96] to make the triangular mesh accurately characterize the essential contour structure. BL2D is a bidimensional, adaptive and anisotropic mesh generator. It uses the Delaunay's method to generate a triangular mesh. In BL2D, the background mesh is an existing mesh applied to generate an adaptive foreground mesh. The foreground mesh is built from the background mesh by an estimator which consists in giving a metric at each point of the background mesh. The metric is represented by a symmetric positive definite matrix with three coefficients (a,b,c). By a rotation at an angle θ making a reference line parallel to one of the two axes of the ellipse, the metric (a,b,c) is easily obtained by the relation

$$\begin{pmatrix} a & b \\ b & c \end{pmatrix} = \begin{pmatrix} \cos\theta & -\sin\theta \\ \sin\theta & \cos\theta \end{pmatrix} \begin{pmatrix} \frac{1}{h_1^2} & 0 \\ 0 & \frac{1}{h_2^2} \end{pmatrix} \begin{pmatrix} \cos\theta & \sin\theta \\ -\sin\theta & \cos\theta \end{pmatrix} \tag{7}$$

where the values h_1 and h_2 represent the desired sizes along two orthogonal directions. As the three quantities (θ,h_1,h_2) are related to the orientation and anisotropy factor of the elements in the adapted triangulation, we can enforce an adaptation of the triangular mesh as follows: (1) setting three quantities according to the function u obtained from the minimizing component at the previous iteration, and (2) building the foreground mesh as a Delaunay triangulation with respect to the metric which is given at each point of the background triangulation, according to above three quantities. Interested reader can refer to [GB98] for detailed description of the building of adaptive mesh.

5.2 The minimizing algorithm

Once a triangulation T is given, we need to minimize $F_\varepsilon(u)$ with respect to u, which is piecewise linear on each element of T and continuous on Ω. In general, standard minimizing techniques may fail due both to the lack of convexity and to the presence of many local minima. In order to ensure that the energy decreases after each iteration, we apply the quasi-Newton algorithm to minimize $F_\varepsilon(u)$. The quasi-Newton algorithm is the most popular algorithms in nonlinear optimization, with a reputation for fast convergence. The most widely used quasi-Newton formula is BFGS. BFGS preserves symmetry and positive definiteness of

the approximation of Hessian matrix, which may be satisfied with a line search using the Wolfe condition. In this paper, we use BFGS formula to approximate the Hessian matrix. Fig.2 shows a flowchart of the minimizing algorithm for the functional $F_\varepsilon(u)$.

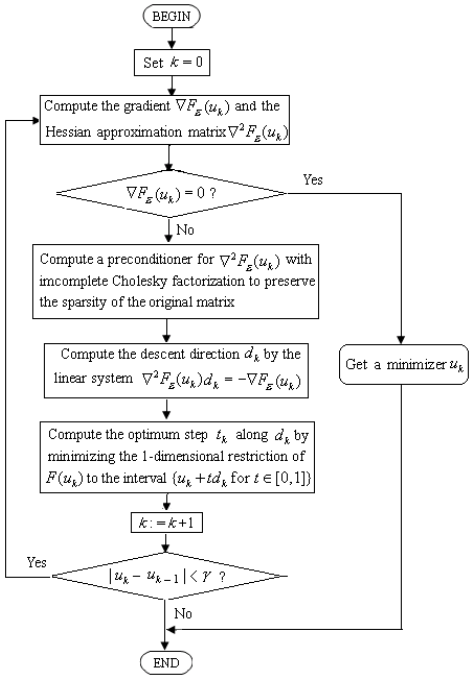

Figure 2: The minimizing algorithm.

6. Experimental results

In this section, we carry out some experiments respectively on a synthetic image (256×256 pixels), and three jacquard images (256×256 pixels) with different types of contours and shapes. The results have been obtained using software written in *C* programming language on the UNIX operating system running on a IPC SUN workstation. In our numerical experiments, we choose the parameters as follows: α =0.1, β = 0.001, γ =2.5×10^{-2}, μ =3.125×10^{-4}, ε =1/256≈0.004. As in practice it is difficult to exactly determine the noise in real images, here we examine the performance of our algorithm by adding "salt and pepper" noise to all the tested images. Fig. 3 illustrates the segmentation result of a synthetic image using our algorithm. Fig. 3 (a) gives a synthetic image with 40% noise. Fig. 3 (b) gives the initial background mesh generated by BL2D. After 8 mesh adaptation processes, the final foreground mesh is shown in Fig. 3 (c). The segmented image and its edge set are shown in Fig. 3 (d) and 3 (e).

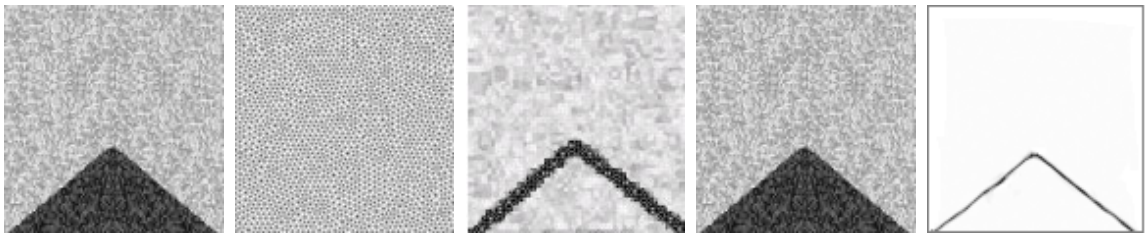

(a) (b) (c) (d) (e)

Figure 3: *Segmentation of a synthetic image with 40% noise. (a) Noisy synthetic image. (b) Initial background mesh. (c) Final foreground mesh. (d) Segmented image. (e) Edge set.*

We measure the order of accuracy for the mesh adaptation algorithm by comparing the length and area error of the triangular-shape in Fig.3 (a) between the analytical solution and numerical solution. Table 1 provides detailed accuracy measurements and shows how the length and area error depends on the mesh size ε . As the mesh size decreases, the adaptive triangular mesh will be more and more approaching the boundary of the triangular-shape.

Mesh size	Length error	Area error
$\varepsilon = 0.004$	0.0549	0.00735
$\varepsilon = 0.002$	0.0287	0.00361
$\varepsilon = 0.001$	0.00878	0.000945
$\varepsilon = 0.0005$	0.00453	0.000455
$\varepsilon = 0.00025$	0.00186	0.000269
$\varepsilon = 0.000125$	0.000944	0.000162
$\varepsilon = 0.0000625$	0.000344	0.0000833
$\varepsilon = 0.00003125$	0.000182	0.0000453

Table 1: *Number of length and area error changes during the mesh adaptation processes.(ε is the greatest length of the edges in the triangulation)*

We also conduct experiments to compare our algorithm with a traditional active contours algorithm, the geometric active contours algorithm (GAC) [MSV95] under different noise environments. Fig. 4 and Fig. 5 illustrate the segmentation results of three jacquard images using the GAC algorithm and our algorithm, respectively. We select three images with different shapes of petals from our jacquard image database. The shapes of petals in Fig. 4 (a)-(c) are roundish, cuspidate and irregular, respectively. Fig. 5 (a)-(c) show the segmentation results of jacquard images in Fig. 4 using the GAC algorithm. Fig. 5 (d)-(f) shows the segmentation results of jacquard images in Fig. 4 using our algorithm after 10 mesh adaptation processes. Comparing with Fig. 5 (a)-(c), sharp boundaries are accurately detected and strengthened in Fig. 5 (d)-(f). They clearly demonstrate the sturdiness of our algorithm when subject to noise. The analysis of the experiment results finds that false detected or missed boundaries are mainly caused by noise occurring on the boundaries, which confuses the detection of boundaries by the GAC algorithm. By this experiment, we also show how our algorithm can be applied to detect edges or other features in contours without gradients, while it is impossible for the GAC algorithm based on the gradient information. Here, we can see that our algorithm is more robust than the GAC algorithm for the segmentation of noise-corrupted jacquard images. Fig. 6 shows the triangular meshes of the pedals in Fig. 5 (d)-(f) which are generated by BL2D.

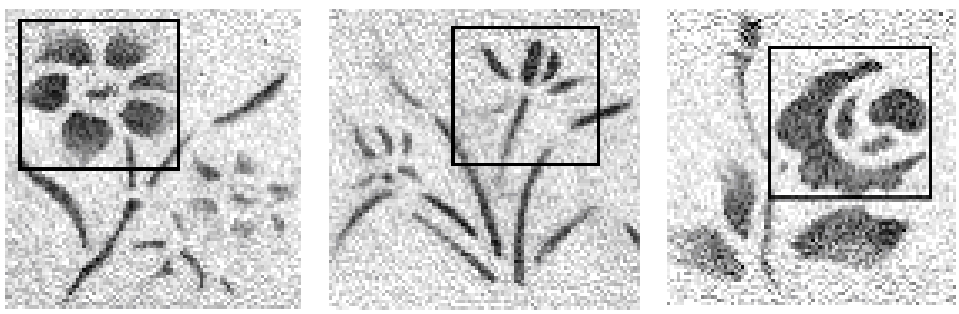

(a) (b) (c)

Figure 4: *Three shapes of petals with 40% noise. (a) roundish. (b) cuspidate. (c) irregular.*

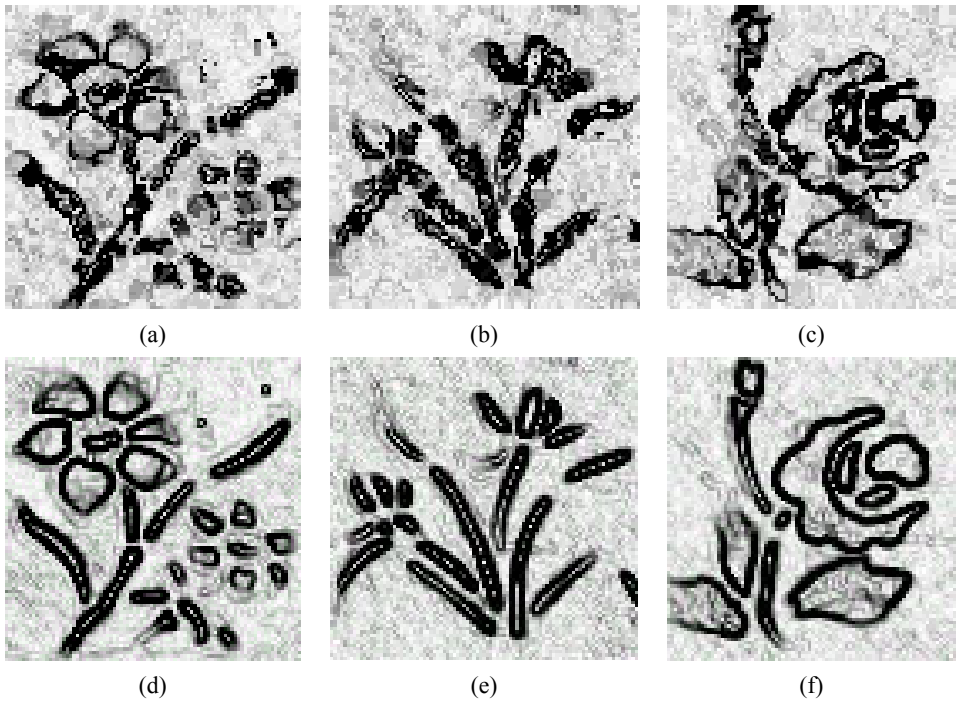

Figure 5: *Segmentation results of jacquard images using two different algorithms. (a) - (c) and (d) - (f) are segmentation results using GAC algorithm and our algorithm, respectively.*

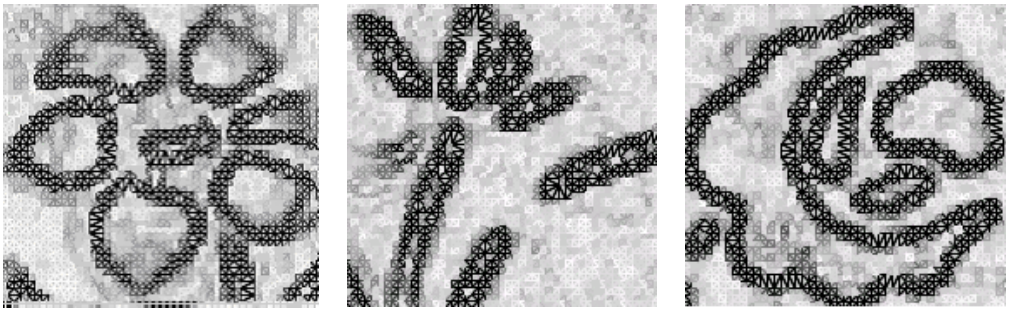

Figure 6: *Triangular mesh generated by BL2D*

In Fig. 7, we give 3-dimenstion plots of the segmented petals in Fig. 4 using two different algorithms. In Fig.8 we give the irregular petals in Fig. 4 (c) with different noise levels from 40% to 80%. In Fig.9, we show some comparisons of topological shape variations of the segmented irregular petals in Fig. 8 using two different algorithms. It can be seen clearly that our algorithm is more suitable for the preservation of topological shapes of petals in each of the three noise levels.

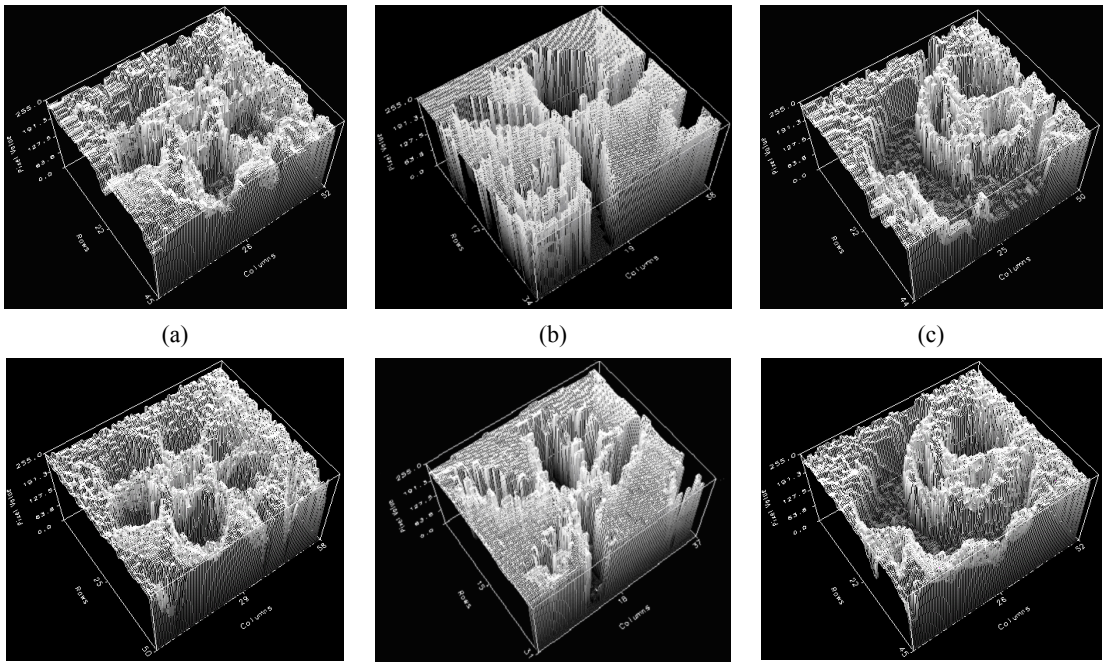

(a) (b) (c)

(d) (e) (f)

Figure 7: *Comparison of segmentation results with 40% noise.(a) - (c) GAC algorithm. (d) - (f) our algorithm.*

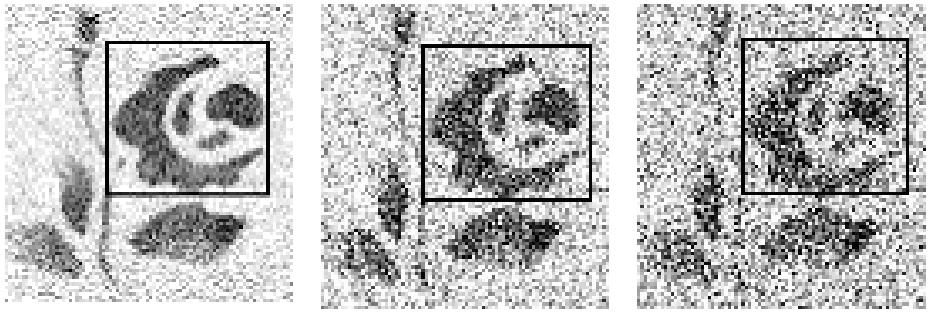

(a) (b) (c)

Figure 8: *The irregular petals with different noise levels. (a) 40% noise. (b) 60% noise. (c) 80% noise*

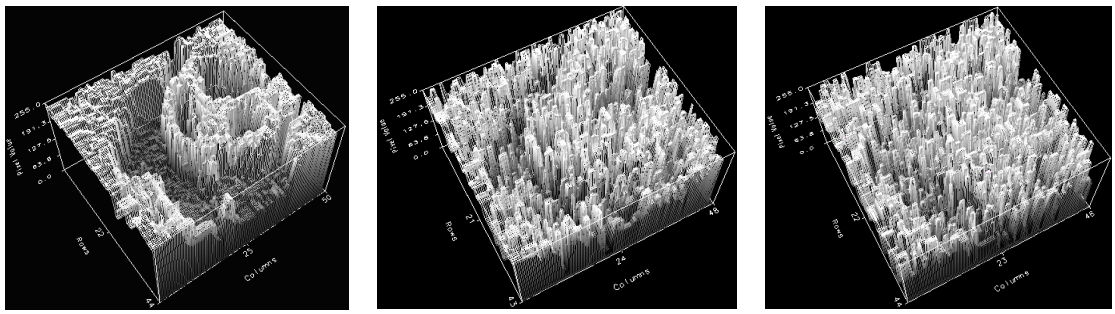

(a) (b) (c)

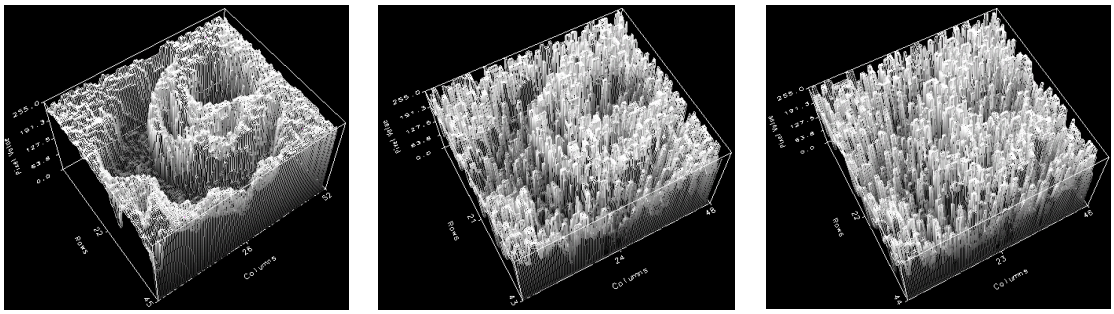

(d) (e) (f)

Figure 9: *Comparison of topological shape variations.(a) GAC algorithm, 40% noise. (b) GAC algorithm, 60% noise. (c) GAC algorithm, 80% noise. (d) Our algorithm, 40% noise. (e) Our algorithm, 60% noise. (f) Our algorithm, 80% noise.*

The following experiments are designed for comparing the accuracy and efficiency of our algorithm with another popular minimizing method for the Mumford-Shah model [CV01]. We adopt two indirect measures to evaluate the objective performance of fine image segmentation: the number of segmented regions, and the mean square error (MSE) between the original and the segmented images. Since MSE represents the degree of segmented region homogeneity for a given number of regions, it can be used as an indirect measure of segmentation efficiency if we consider the number of regions simultaneously. The segmentation results in Table 2 demonstrate that the proposed algorithm improves the fine segmentation performance since it produces better objective segmentation quality in terms of MSE even with a smaller number of regions compared with the algorithm proposed by Chan *et al*.

	Chan *et al*.'s algorithm		Proposed algorithm	
	Number of regions	MSE	Number of regions	MSE
Fig.4 (a)	460	49.65	405	36.87
Fig.4 (b)	540	43.22	470	37.58
Fig.4 (c)	490	40.35	420	30.26

Table 2: *Number of regions and MSE comparison between the Chan et al.'s algorithm and the proposed algorithm*

Table 3 shows the comparison of computational time between the Chan *et al*.'s algorithm and the proposed algorithm. We can see that the two models spend the same iteration time to accomplish the segmentation process, but the proposed algorithm consumes much less time than the algorithm proposed by Chan *et al*. in each iteration.

	Chan *et al*.'s algorithm		Proposed algorithm	
	Iteration times	Average time of iteration	Iteration times	Average time of iteration
Fig.4 (a)	40	0.557	40	0.432
Fig.4 (b)	50	0.578	50	0.480
Fig.4 (c)	70	0.515	70	0.418

Table 3: *Computational time comparison between the Chan et al.'s algorithm and the proposed algorithm*

7. Conclusions

In summary, we have presented a novel algorithm for jacquard image segmentation based on the Mumford-Shah model. For solving the corresponding minimization problem, an iterative relaxation algorithm is proposed. The proposed algorithm is applied to segment noisy jacquard images and shows its capability of accurate segmentation. Experimental results show that the proposed algorithm enhances its resistance to noise, so that the drawback of the active contour methods being easily affected by noise is greatly improved. Future work would look into learning patterns of variability from a training set and exploiting prior knowledge to provide more robust and accurate results.

References

[AT90] AMBROSIO L., TORTORELLI V. M.: Approximation of functionals depending on jumps by elliptic functionals via Gamma-convergence.

Comm. Pure Appl. Math (1990), vol. 43, pp. 999-1036.

[BL96] BOROUCHAKI H., LAUG, P.: *The bl2d mesh generator: Beginner's guide, user's and programmer's manual* (1996). Technical Report RT-0194, INRIA.

[Cha95] CHAMBOLLE A.: Image segmentation by variational methods: Mumford and Shah functional and the discrete approximations. *SIAM J. Appl. Math.* (1995), vol. 55, pp. 827-863.

[CRB99] CHESNAUD C., REFREGIER P., BOULET V.: Statistical region snake-based segmentation adapted to different physical noise models. *IEEE Trans.Pattern Analysis and Machine Intelligence* (1999), vol. 21, pp.:1145-1157.

[CV01] CHAN T. F., VESE L.: A level set algorithm for minimizing the Mumford-Shah functional in image processing. In *proc*. "Variational and Level Set Methods in Computer Vision" (2001), 161–168.

[Dal93] DAL M. G.: *An introduction to Γ-convergence*. Birkhäuse, 1993.

[DCL90] De GIORGI E., CARRIERO M., LEACI A.: Existence theorem for a minimum problem with free discontinuity set. *Arch. Rational Mech. Anal* (1990), vol. 111, pp.291-322.

[GB98] GEORGE P.L, BOROUCHAKI H.: *Delaunay triangulation and meshing: application to finite elements*. Hermes, 1998.

[Gob98] GOBBINO M.: Finite difference approximation of the Mumford-Shah functional. *Comm. Pure Appl. Math* (1998), vol. 51, pp.197-228.

[KWT87] KASS M., WITKIN A., TERZOPOULOS D.: Snakes: active contour models. *Int. J. Computer. Vis* (1987), vol.1, pp.321-331.

[MGR04] MARTIN P., GOUDAIL F., REFREGIER P.: Influence of the Noise Model on Level Set Active Contour Segmentation. *IEEE Trans.Pattern Analysis and Machine Intelligence* (2004), vol. 26, pp. 799-803.

[MS89] MUMFORD D., SHAH J.: Optimal approximations by piecewise smooth functions and associated variational problems. *Comm. Pure Appl. Math.* (1989), vol. 42, pp. 577-685.

[MSV95] MALLADI R., SETHIAN J. A., Vemuri B. C.: Shape modeling with front propagation: A level set approach. *IEEE Trans.Pattern Analysis and Machine Intelligence* (1995), vol. 17, pp. 158-175.

[Neg99] NEGRI M.: The anisotropy introduced by the mesh in the finite element approximation of the Mumford-Shah Functional. *Numer. Funct. Anal. Optim* (1999), vol. 20, pp. 957-982.

[TYW01] TSAI A., YEZZI A., WILLSKY A.S.: Curve evolution implementation of the Mumford-Shah functional for image segmentation, denoising, interpolation, and magnification. *IEEE Trans.Image Processing* (2001), vol. 10, pp. 1169-1186.

[ZHPZ96] ZHUANG X.H., HUANG Y., PALANIAPPAN K., ZHAO Y.X.: Gaussian mixture density modeling, decomposition, and applications. *IEEE Trans.Image Processing* (1996), vol. 5, pp. 1293-1302.